

Creep control in soft particle packings.

Joshua A. Dijksman^{1,*} and Tom Mullin^{2,†}

¹*Physical Chemistry and Soft Matter, Wageningen University & Research, Stippeneng 4, 6708 WE Wageningen, The Netherlands*

²*The Mathematical Institute and Linacre College, University of Oxford.OX2 6GG,U.K.*

(Dated: May 12, 2022)

Granular packings display a wealth of mechanical features which are of widespread significance. One of these features is creep: the slow deformation under applied stress. Creep is common for many other amorphous materials such as many metals and polymers. The slow motion of creep is challenging to understand, probe and control. We probe the creep properties of packings of soft spheres with a sinking ball viscometer. We find that in our granular packings, creep persists up to large strains and has a power law form, with diffusive dynamics. The creep amplitude is exponentially dependent on both applied stress and the concentration of hydrogel, suggesting that a competition between driving and confinement determines the dynamics. Our results provide insights into the mechanical properties of soft solids and the scaling laws provide a clear benchmark for new theory that explains creep, and provide the tantalizing prospect that creep can be controlled by a boundary stress.

The mechanical properties of athermal particle packings are of fundamental and applied interest and have various non-trivial features. Many systems such as sand, foams, emulsions and other particulate media have a “rigid” phase that can bear a finite amount of stress [1–10]. However, the definition of “rigid” is not always clear, for example because of slow mechanical motion or *creep* in thermally driven amorphous materials [11]. Packings of inelastic particles might be considered rigid, yet they also display slow relaxation dynamics when *deformation* is imposed, even in the absence of thermal fluctuations; they are considered to self-fluidize [12, 13]. Alternatively, when *stress* is imposed, granular packings also display very small magnitude logarithmic aging [14, 15]. Hence, the origin of creep in athermal packings is obscure.

In this letter we show that athermal soft sphere packings display readily observed, large amplitude creep behavior when the applied stress of the intruder and the packing characteristics are controlled systematically. Observed creep behavior is diffusive in time, robustly observed under different experimental conditions and depends exponentially on the applied intruder stress. Our work shows that creep behavior can be systematically studied, which opens the door to finding the new physics needed to understand the slow flow behavior of (a)thermal particle packings. Specifically, our work suggests that creep features are set by a balance of applied and confinement stress and originate in particle or contact level details.

Microscopic details are always relevant to the understanding of the properties of soft solids. For example, it is known that constraining the various internal degrees of freedom of particles leads to rigidity in idealized structures [3, 16], e.g. where contacts proliferate. However, the properties of the rigid state also depend on the mi-

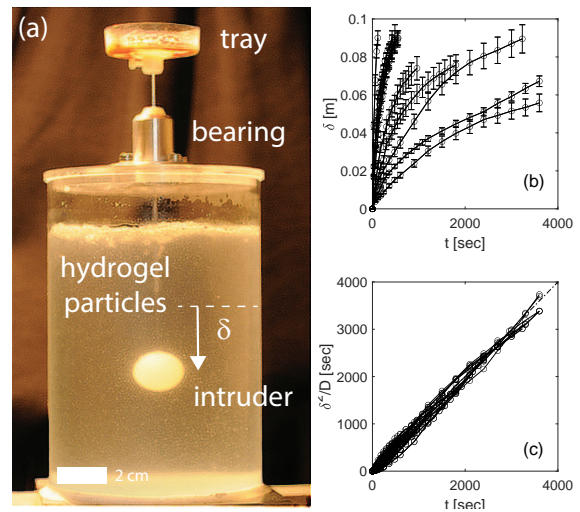


Figure 1. (a) Photo of the experimental setup with various parts indicated. δ is the penetration depth measured from a reference point (dashed line) which is always below the surface of the packing. (b) Penetration depth δ as a function of time for various hydrogel concentrations and added weights. Error bars indicate measurement uncertainty on the position. (c) δ^2 dynamics normalized with fitted D values (see text) for all penetration tests. The dash-dotted line indicates a slope of unity.

croscopic details of the particle contacts and adhesion, size, aspect ratio, boundary conditions, sample preparation and the way the rigidity of the assembly is probed. Controlling for all these variables is a huge challenge and a framework to understand rigidity is lacking in no small part due to the experimental challenges in systematically probing creep behavior. We therefore consider the classic viscosity test of a sinking intruder of known shape and size and tunable effective density to probe the mechanical properties of packings of soft particles.. The medium

we use is a dense packing of millimeter sized hydrogel spheres. In essence, we use the principles of a falling bob viscometer to study the properties of hydrogel particles packings. Such viscometers are commonly used to obtain estimates of the viscosity of Newtonian fluids [17], or non-Newtonian fluids [18, 19]. Viscoelastic fluids such as Boger fluids have been treated extensively, yet also “simple” yield stress fluids have been studied using sphere intrusion [20–22].

Unlike their microgel equivalents [23], saturated millimeter sized soft hydrogel particles do not easily change volume under small pressures [24–26] and can be easily confined to a constant pressure or volume. They are known to have non-Newtonian flow behavior, even sans submersion [27]. Hydrogels are virtually frictionless [28, 29] when fully immersed in water. Even so, a packing of frictionless spheres is known to have a yield stress [22, 28, 30], signalling its rigid feature. The macroscopic size of our system was selected to enable accurate mechanical control. The intruder is much larger than the particle scale and thus provides a coarse-grained measure of the packing mechanics.

Principle creep phenomenology — Spheres sinking into a non-Newtonian fluid typically exhibit behaviour ranging from unsteady motion to arrest. Our experiments yield qualitatively different behaviors. (i) The sinking dynamics of the sinking sphere in the hydrogel particle packing does not stop [31]; it creeps with reproducible power law time dependence. It is important to distinguish between the “creeping flow” limit of inertia free dynamics, and “creep flow”, which is slow, inertia free motion that is nevertheless not steady due to ageing [32]. (ii) The creep becomes exponentially dependent on the applied stress [33, 34] at a critical fraction of hydrogel material per unit volume ρ_c . (iii) Increasing the hydrogel concentration further, we find a transition from creep to “creeping” sinking behavior at a hydrogel concentration ρ_l while retaining its exponential stress dependence.

Experiments — The experimental apparatus is presented in Fig. 1a. We use an acrylic cylinder which contains a prepared packing of hydrogel spheres. The packing of hydrogel spheres can be adjusted by adding small measured amounts of dry hydrogel powder. An intruder is guided into the packing by an attached rod, that serves as a measure to track the penetration $\delta(t)$ into the medium. The rod also supports a tray, to which calibrated masses are added. At the start of each experiment the rod is held fixed using a clamp. The initial position of the intruder δ_0 is with the top of the intruder positioned totally immersed, 5 mm below the sample surface. The experiment is started by releasing the clamp. The total stress σ exerted by the intruder on the packing is computed using the total weight of intruder, rod, tray and added mass, divided by the cross section of the intruder. Note that this is a normal stress, computed with the cross section of the intruder. Details regarding the

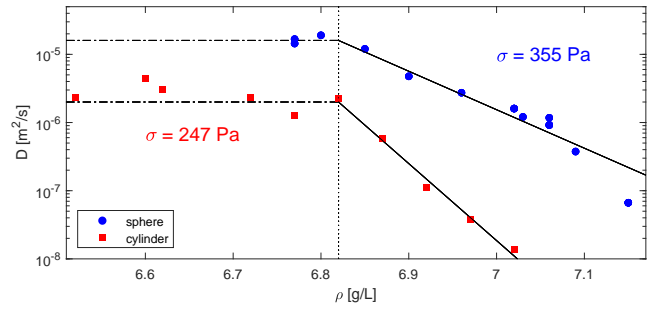


Figure 2. At constant stress, we measure $D(\rho)$ for the 23 mm sphere (blue circles) and the 30 mm cylinder (red squares) at constant sinking stress σ of having no weights in the tray. The dash-dotted line indicates regime of density-independent creep; the solid line indicates density dependent creep intrusion dynamics. The dotted line indicates ρ_c .

experiment can be found in the supplementary material [url], which describes the methods to prepare the samples and some other details and includes [35–37].

Creep features — The salient feature of the mechanics of the weak hydrogel particle packings is that they exhibit power law creep over a wide range of hydrogel concentrations and applied stress. Results for $\delta(t) = (D(\rho, \sigma)t)^{0.5}$ from sphere intrusion dynamics are shown in Fig. 1b for various σ, ρ . D here is a diffusion-like constant with units of m^2/s that sets the penetration speed. The unsteady penetration dynamics is present in all experimental runs and persists for hours. We focus first on the sphere intrusion with no added weights in the tray which corresponds to a constant stress of approximately 360 Pa. The square root time dependence of δ is evidenced by plotting $\delta^2(t)$ normalised by the fitted $D(\rho, \sigma)$ as shown in Fig. 1c. In fact we obtain $D(\sigma, \rho)$ from a linear fit to $\delta^2(t)$. All the data collapse onto a straight line with slope 1. See supplementary material for a logarithmic comparison of the same data. It should be noted that the distance over which creep persists is up to four times the intruder size. The change in creep behavior at ρ_c is readily observed in $D(\rho)$. Below a critical hydrogel concentration of 6.82 g/L, creep behavior exists with the same power law time dependence, yet D is independent of ρ and can be indicated by D_0 . Above ρ_c , D decays exponentially with ρ as visible in Fig. 2, where we can write:

$$D = D_0 \exp(-(\rho - \rho_c)/\rho_s). \quad (1)$$

Here ρ_s is a decay constant that we fitted to the data. We find that for the sphere, $\rho_s \approx 1/13$ g/L. This $D(\rho)$ behavior is also found for cylindrical intruders, for which $\delta(t)$ also has a square-root fit. The constant D regime is more extensively surveyed with cylindrical intruders; for the 30 mm cylinder $\rho_s \approx 1/26$ g/L. Independent measurements with a larger cylindrical intruder show similar exponential $D(\rho)$ behavior (not shown). Remarkably, we thus see that a packing of hydrogel spheres behaves as a

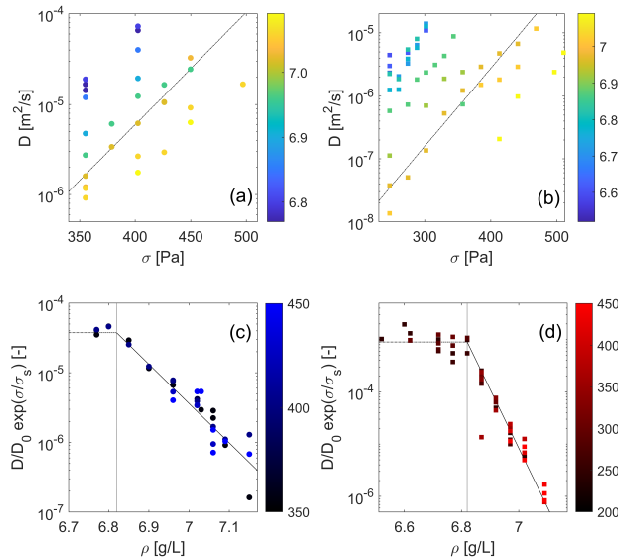


Figure 3. Varying the intruder stress on the packing, (a,c) $D(\rho, \sigma)$ for the 23 mm sphere and (b,d) for the 30 mm cylinder. (a,b) show the exponential intruder stress dependence. The dash-dotted line is $D \propto \exp(\sigma/\sigma_s)$. Color scale indicates the hydrogel concentration. In (c,d) we rescale the data with Eq. 2. Color scale indicates the applied stress σ in Pa. Line styles are identical to Fig. 2.

soft solid that shows creep over the entire range of $\rho < \rho_l$ studied. The creep is reminiscent of thermally activated materials such as polymers and glasses but also found in harder particulate media [14, 38–41].

Intruder stress dependence — Increasing the applied stress σ by adding weights to the tray increases the penetration speed. We find an exponential enhancement of D_0 with stress, as shown in Fig. 3a,b. In this exponential dependence, a stress scale σ_s quantifies how creep changes with applied stress. For both spheres (panel a) and cylinders (panel b), D increases exponentially with the same stress scale $\sigma_s \approx 35$ Pa and indeed the data collapse of $D/D_0 \exp(\sigma/\sigma_s)$ is excellent, especially above ρ_c . Normalizing D by $D_0 \exp(\sigma/\sigma_s)$ does not scale out the diffusion amplitude entirely. We therefore conclude that the overall prefactor D_0 can be described as

$$D_0 = D_\sigma \exp(\sigma/\sigma_s) \quad (2)$$

Here D_σ is a geometry dependent factor with $D_\sigma \approx 3.5 \times 10^{-3}$ m²/s for the spheres and $D_\sigma \approx 9 \times 10^{-4}$ m²/s for the cylinders. As the sphere is only 1.5 times smaller than the cylinder, we expect the remaining difference in D_σ to arise from geometric effects: the flat face of the cylinder pushes small numbers of particles along, effectively changing its shape.

Interpretation — The remarkable stress dependence observed by varying the effective mass and the hydrogel

concentration suggests a mechanism connects the two effects. Indeed, the scaling for D in the regime $\rho_c < \rho < \rho_l$ is

$$D = D_\sigma \exp\left(\frac{\sigma}{\sigma_s} - \frac{(\rho - \rho_c)}{\rho_s}\right). \quad (3)$$

It seems more natural to see the diffusion constant as a balance of two competing stresses. First, ρ_c is intruder shape independent, so it is a property of the packing. We observe that the fully hydrated, swollen hydrogel particles start to protrude through the water surface when the hydrogel concentration has reached ρ_c . We interpret ρ_c as the hydrogel particle concentration at which the number of swollen hydrogel spheres fills the available volume of water. When dry hydrogel powder is added to an already completely filled liquid volume of water, particles swell to a hydrated state and protrusion increases. Surface tension then becomes relevant as the confining stress for the hydrogel particles. The surface tension stress is $2\gamma/d$ with γ the surface tension and d the average particle diameter, and yields about 100 Pa. This value is larger than the measured value for the geometry independent σ_s but closer to this value than the other stress scale in the system: hydrostatic pressure. With 6g/L hydrogel, where the maximum hydrostatic pressure is $\Delta\rho gh \approx 12$ Pa with h the packing height of about 20 cm. We conclude that creep speed appears to be set by the ratio of driving stress from intruder mass and the confining stress from the surface tension. Preliminary experiments suggest that adding a surfactant can increase D at given ρ , but more work is needed to quantify these effects.

Origin of geometry dependent prefactor D_σ — On dimensional grounds, in the creep regime, since D_σ has the units of a diffusion constant m²/s, this implies it will depend on a characteristic stress scale σ of the intruder, on a density or concentration ρ and a length scale L via $D_\sigma \propto L\sqrt{\sigma/\rho}$. σ_s is universal, hence a natural stress scale, the more so since the hydrostatic pressure scale is both too small and depth dependent and thus unlikely to produce the observed creep dynamics. While our experiment is limited in the exploration of different sizes, shapes and material densities, we find that ρ_s and D_σ are intruder dependent and thus likely related. However, the value of ρ_c, ρ_s requires careful interpretation, as the dry hydrogel weight per unit of volume of water is a proxy for the collective dynamics of the swollen hydrogel particles. Having established the values of ρ , we can estimate $L \approx D_\sigma \sqrt{\rho_s/\sigma_s}$ and find that $L \approx 1$ -2mm, which is equal to the particle size. The appearance of this length scale is consistent with the surface tension argument above, which would indeed include surface tension parameters in the effective prefactor D_σ . The relevance of surface tension for the creep behavior also provides an interpretation for the geometry dependent ρ_s : this constant is

related to the amount of Reynolds dilatancy the packing of hydrogel particles experiences under the motion of the intruder. ρ_s for the cylinder is thus also much smaller. It is interesting to observe the creep and its exponential dependence on both ρ and σ . Preliminary flow field visualizations rule out an emerging and compressing solid-like region underneath the intruder; the flow field during penetration is known to be limited around the sphere [22, 42]. Moreover, creep is consistently observed for both intruder shapes. We postulate that the soft hydrogel packing acts as an athermal glass former [43] in which *any* motion of the intruder destabilizes the packing and induces fluidization, which gives rise to motion. The self-fluidization will be suppressed under larger confining pressure, or enhanced when the driving pressure is higher. We cannot probe the limit $\sigma \rightarrow 0$ so we are unable to verify whether the self-fluidization persists to the point where the material becomes a “solid”, yet if Eq. 2 extends to infinitesimal stress levels, our observations indicate that frictionless, deformable particles allow minute mechanical fluctuations to liquefy a packing of jammed particles. The anti-thixotropy [44] or aging phenomenon observed fits remarkably well in the framework from Derec *et al* [37], with an aging exponent $\alpha = 3$ (see supplementary material).

Robust σ_s dependence in viscous sinking — The diffusive penetration dynamics does not extend to arbitrarily large hydrogel concentrations, but the stress dependent dynamics does. At a transition hydrogel concentration $\rho = 7.15$ g/L we observe a mixed sinking behavior that cannot be described by unsteady creep with a single exponent. Upon increasing $\rho > 7.15$ gr/L we enter a third regime. In this regime, the sphere sinks at a constant speed. Typical $\delta(t)$ behavior is shown in Fig. 4a and contrasts starkly with the creep behavior in Fig. 1b. Here we fit $\delta = v_s t$ and using Stokes drag law we find that $v_s = 4R^2 g \Delta\rho / 18\eta_{\text{eff}}$, with R the intruder radius, η_{eff} the effective viscosity of the hydrogel packing and $\Delta\rho$ the density difference between the intruder + weights and the water-hydrogel mixture. The $\eta_{\text{eff}}(\rho)$ dependence is weak but a slowdown with increasing hydrogel concentration can be observed, as can be seen in Fig. 4b. In a simple fluid the speed of intrusion varies linearly with added mass and hence σ , but the dependence on stress is significantly stronger, as is D_σ . We clarify this in Fig. 4c where we show various $v_s(\sigma)$ at constant $\rho = 7.45$ g/L. Again, an exponential dependence of the effective viscosity on the stress can be seen. The reference line shown follows Eq. 2 and has the same σ_s as used for describing D below ρ_l suggesting a robust stress dependence across regimes.

Conclusions — By varying the intruder stress and amount of hydrogel particles in a fixed volume of water, we find that creep in athermal soft particle packings can be systematically observed and depends exponentially on the intruder stress under a wide range of conditions. We

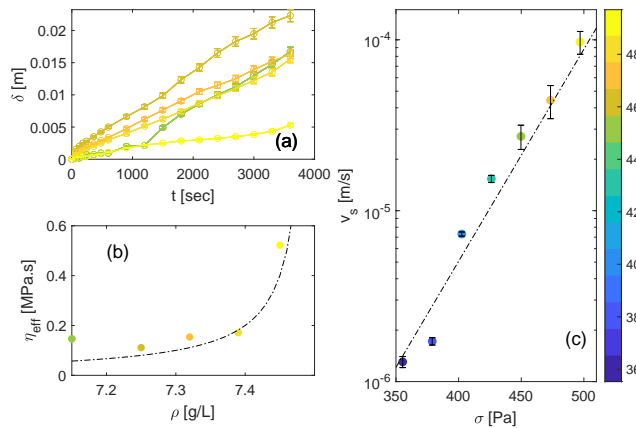


Figure 4. (a) Above ρ_l , penetration depth δ as a function of time for various hydrogel concentrations at constant stress $\sigma = 358$ Pa. (b) the effective viscosity as derived from the sinking speed v_s . Color indicates ρ . The dash-dotted line shows a $\eta_{\text{eff}} \propto 1/(7.5 - \rho)$ divergence as guide to the eye. (c) v_s as a function of stress σ . At fixed $\rho = 7.45$ g/L, v_s is approximately exponential; the dash-dotted line is given by $v_s \propto \exp(\sigma/\sigma_s)$. σ is indicated by the color scale, in Pa. Error bars indicate the 95% confidence interval of the fit.

find three regimes of sinking dynamics: (i) a regime with power law intrusion creep with an exponent of 0.5 for the penetration versus time dynamics, in which the hydrogel concentration does not affect the sinking speed prefactor. (ii) A second regime with the same power law intrusion creep in which the speed is exponentially dependent on the packing and the distance to a critical volume fraction. (iii) a regime of constant sinking rate. The observations are robust for different intruder shapes. We interpret the observed exponential stress dependence from a balance of driving stress and confinement pressure induced by surface tension and link the observed power law creep to a different type of aging than commonly found in logarithmic creep experiments. Our results provide a clear challenge for numerical and theoretical work. The observed exponential stress dependence provides a test for existing frameworks of particle packing mechanics and point towards a relevance of understanding particle contact level physics and boundary conditions on the fluctuations in granular packings to arrive at coarse grained level descriptions of disordered particulate media. Our extensive set of experimental results prompt several questions: which mechanism allows for the creep phenomenon? What sets the observed stress scale? Is a boundary stress indeed responsible for the local flow behavior? Our data so provides a benchmark for perspectives proposed for mechanics in athermal packings [45–48] and will stimulate new experimental and theoretical work in the field.

The experiments were initiated in the Observatory in the Mathematical Institute at Oxford University. The majority of the experiments were completed in TM’s

house during lockdown. TM's wife, Sylvia is thanked for her forbearance. TM is grateful to Dominic Vella and Lucie Domino for their support. The authors are also grateful to Keith Long who manufactured the apparatus. Chandan Shakya is thanked for carrying out preliminary experiments on the rheology and flow behavior of hydrogel suspensions. We thank Iker Zuriguel and Jorge Peixinho for providing useful feedback. JAD acknowledges funding from the European Union's Horizon 2020 research and innovation program under the Marie Skłodowska Curie grant agreement No 812638.

* joshua.dijksman@wur.nl

† tom.mullin@maths.ox.ac.uk

- [1] Ian D. Evans and Alexander Lips. Concentration dependence of the linear elastic behaviour of model microgel dispersions. *Journal of the Chemical Society, Faraday Transactions*, 86(20):3413, 1990. Publisher: Royal Society of Chemistry (RSC).
- [2] E. Bartsch, T. Eckert, C. Pies, and H. Sillescu. The effect of free polymer on the glass transition dynamics of microgel colloids. *J. Non-Cryst. Solids*, 307–310:802–811, 2002.
- [3] M. van Hecke. Jamming of soft particles: geometry, mechanics, scaling and isotaticity. *Journal of Physics: Condensed Matter*, 22(3):033101, December 2009. Publisher: IOP Publishing.
- [4] Zhen Shao, Ajay Singh Negi, and Chinedum O. Osuji. Role of interparticle attraction in the yielding response of microgel suspensions. *Soft Matter*, 9(22):5492, 2013. Publisher: Royal Society of Chemistry (RSC).
- [5] Dimitris Vlassopoulos and Michel Cloitre. Tunable rheology of dense soft deformable colloids. *Current Opinion in Colloid & Interface Science*, 19(6):561 – 574, 2014.
- [6] Ph Coussot. Yield stress fluid flows: A review of experimental data. *Journal of Non-Newtonian Fluid Mechanics*, 211:31–49, 2014.
- [7] Anindita Basu, Ye Xu, Tim Still, PE Arratia, Zexin Zhang, KN Nordstrom, Jennifer M Rieser, JP Gollub, DJ Durian, and AG Yodh. Rheology of soft colloids across the onset of rigidity: scaling behavior, thermal, and non-thermal responses. *Soft matter*, 10(17):3027–3035, 2014.
- [8] Massimiliano M. Villone and Pier Luca Maffettone. Dynamics, rheology, and applications of elastic deformable particle suspensions: a review. *Rheologica Acta*, 58(3-4):109–130, April 2019.
- [9] Christopher S O'Bryan, Christopher P Kabb, Brent S Sumerlin, and Thomas E Angelini. Jammed polyelectrolyte microgels for 3d cell culture applications: rheological behavior with added salts. *ACS Applied Bio Materials*, 2(4):1509–1517, 2019.
- [10] Heather M Shewan, Gleb E Yakubov, Mauricio R Bonilla, and Jason R Stokes. Viscoelasticity of non-colloidal hydrogel particle suspensions at the liquid–solid transition. *Soft Matter*, 17(19):5073–5083, 2021.
- [11] Edward Neville Da Costa Andrade. On the viscous flow in metals, and allied phenomena. *Proceedings of the Royal Society of London. Series A, Containing Papers of a Mathematical and Physical Character*, 84(567):1–12, 1910.
- [12] P. Hébraud and F. Lequeux. Mode-coupling theory for the pasty rheology of soft glassy materials. *Phys. Rev. Lett.*, 81:2934–2937, Oct 1998.
- [13] Lydéric Bocquet, Annie Colin, and Armand Ajdari. Kinetic theory of plastic flow in soft glassy materials. *Phys. Rev. Lett.*, 103:036001, Jul 2009.
- [14] Van Bau Nguyen, Thierry Darnige, Ary Bruand, and Eric Clement. Creep and fluidity of a real granular packing near jamming. *Phys. Rev. Lett.*, 107:138303, Sep 2011.
- [15] Nakul S Deshpande, David J Furbish, Paulo E Arratia, and Douglas J Jerolmack. The perpetual fragility of creeping hillslopes. *Nature Communications*, 12(1):1–7, 2021.
- [16] Christopher R Calladine. Buckminster fuller's "tensegrity" structures and clerk maxwell's rules for the construction of stiff frames. *International journal of solids and structures*, 14(2):161–172, 1978.
- [17] Tom E Faber. *Fluid dynamics for physicists*. Cambridge university press, 1995.
- [18] AN Beris, JA Tsamopoulos, RC Armstrong, and RA Brown. Creeping motion of a sphere through a bingham plastic. *Journal of Fluid Mechanics*, 158:219–244, 1985.
- [19] Gareth H McKinley. Steady and transient motion of spherical particles in viscoelastic liquids. *Transport Processes in Bubble, Drops, and Particles*, pages 338–375, 2002.
- [20] Blandine Gueslin, Laurence Talini, Benjamin Herzhaft, Yannick Peysson, and Catherine Allain. Flow induced by a sphere settling in an aging yield-stress fluid. *Physics of Fluids*, 18(10):103101, 2006.
- [21] Jean-Michel Piau. Carpopol gels: Elastoviscoplastic and slippery glasses made of individual swollen sponges: Meso-and macroscopic properties, constitutive equations and scaling laws. *Journal of non-newtonian fluid mechanics*, 144(1):1–29, 2007.
- [22] Rausan Jewel, Andreea Panaitescu, and Arshad Kudrolli. Micromechanics of intruder motion in wet granular medium. *Phys. Rev. Fluids*, 3:084303, Aug 2018.
- [23] Felix A Plamper and Walter Richtering. Functional microgels and microgel systems. *Accounts of chemical research*, 50(2):131–140, 2017.
- [24] Shengqiang Cai and Zhigang Suo. Mechanics and chemical thermodynamics of phase transition in temperature-sensitive hydrogels. *Journal of the Mechanics and Physics of Solids*, 59(11):2259–2278, 2011.
- [25] Christian Fenger, Lukas Arens, Harald Horn, and Manfred Wilhelm. Desalination of seawater using cationic poly (acrylamide) hydrogels and mechanical forces for separation. *Macromolecular Materials and Engineering*, 305(10):2000383, 2020.
- [26] Jean-François Louf, Nancy B Lu, Margaret G O'Connell, H Jeremy Cho, and Sujit S Datta. Under pressure: Hydrogel swelling in a granular medium. *Science Advances*, 7(7):eabd2711, 2021.
- [27] Kirsten Harth, Jing Wang, Tamás Börzsönyi, and Ralf Stannarius. Intermittent flow and transient congestions of soft spheres passing narrow orifices. *Soft Matter*, 16(34):8013–8023, 2020.
- [28] Marcel Workamp and Joshua A Dijksman. Contact tribology also affects the slow flow behavior of granular emulsions. *Journal of Rheology*, 63(2):275–283, 2019.

- [29] Nicholas L Cuccia, Suraj Pothineni, Brady Wu, Joshua Méndez Harper, and Justin C Burton. Pore-size dependence and slow relaxation of hydrogel friction on smooth surfaces. *Proceedings of the National Academy of Sciences*, 117(21):11247–11256, 2020.
- [30] Pierre-Emmanuel Peyneau and Jean-Noël Roux. Frictionless bead packs have macroscopic friction, but no dilatancy. *Physical review E*, 78(1):011307, 2008.
- [31] M. Siebenbürger, M. Ballauff, and Th. Voigtmann. Creep in colloidal glasses. *Phys. Rev. Lett.*, 108:255701, Jun 2012.
- [32] Leendert Cornelis Elisa Struik. Physical aging in amorphous polymers and other materials, 1977.
- [33] John M. Hutchinson. Physical ageing of polymers. *Prog. Polym. Sci.*, 20:703–760, 1995.
- [34] Pierre Lidon, Louis Villa, and Sébastien Manneville. Power-law creep and residual stresses in a carbopol gel. *Rheologica Acta*, 56(3):307–323, 2017.
- [35] Oxford Water Works & Sewer Board. Annual water quality report. 2021.
- [36] P Ladenburg. On the influence of the walls on the dynamics of a sphere in a flowing fluid. *Ann. Phys*, 23:447–458, 1907.
- [37] Caroline Derec, Armand Ajdari, and Francois Lequeux. Rheology and aging: A simple approach. *The European Physical Journal E*, 4(3):355–361, 2001.
- [38] HM Jaeger, Chu-heng Liu, and Sidney R Nagel. Relaxation at the angle of repose. *Physical Review Letters*, 62(1):40, 1989.
- [39] Gianfranco D’Anna, P Mayor, A Barrat, V Loreto, and Franco Nori. Observing brownian motion in vibration-fluidized granular matter. *Nature*, 424(6951):909–912, 2003.
- [40] Joshua A Dijkstra, Geert H Wortel, Louwrens TH van Dellen, Olivier Dauchot, and Martin van Hecke. Jamming, yielding, and rheology of weakly vibrated granular media. *Physical review letters*, 107(10):108303, 2011.
- [41] Caroline Hanotin, S Kiesgen De Richter, Philippe Marchal, Laurent J Michot, and Christophe Baravian. Vibration-induced liquefaction of granular suspensions. *Physical review letters*, 108(19):198301, 2012.
- [42] B Gueslin, L Talini, and Y Peysson. Sphere settling in an aging yield stress fluid: link between the induced flows and the rheological behavior. *Rheologica acta*, 48(9):961, 2009.
- [43] L Andrew Lyon and Alberto Fernandez-Nieves. The polymer/colloid duality of microgel suspensions. *Annual review of physical chemistry*, 63:25–43, 2012.
- [44] Ronald G Larson and Yufei Wei. A review of thixotropy and its rheological modeling. *Journal of Rheology*, 63(3):477–501, 2019.
- [45] M.-Carmen Miguel, Alessandro Vespignani, Michael Zaiser, and Stefano Zapperi. Dislocation jamming and andrade creep. *Phys. Rev. Lett.*, 89:165501, Sep 2002.
- [46] Pinaki Chaudhuri, Ludovic Berthier, and Srikanth Sastri. Jamming transitions in amorphous packings of frictionless spheres occur over a continuous range of volume fractions. *Phys. Rev. Lett.*, 104:165701, Apr 2010.
- [47] Leonardo E Silbert. Jamming of frictional spheres and random loose packing. *Soft Matter*, 6(13):2918–2924, 2010.
- [48] Suzanne M Fielding. Elastoviscoplastic rheology and aging in a simplified soft glassy constitutive model. *Journal of Rheology*, 64(3):723–738, 2020.

Supplemental Materials

Experimental details — The main component of the experimental setup is a 200 mm long extruded and machined acrylic cylinder which has a 130 ± 1 mm outer diameter and wall thickness 3 mm. A tight fitting lid prevents evaporation and contains a central PTFE bearing through which a rod passes that is connected to the intruders. The bottom 10 mm of the rod is threaded to match the hole in the centre of the intruder. To increase the applied stress σ on the packing, a 55 mm diameter \times 10 mm high acrylic tray is attached to the rod, to which calibrated masses can be added. We use two different intruder shapes: a polypropylene sphere of 23 mm diameter with density 913 kg/m^3 . Note that the polypropylene sphere connected to the rod and tray has an effective density higher than water. We also use plexiglas cylinders with a diameter of 30 mm and 35 mm and length 20 mm and density $\rho_p = 1190 \text{ kg/m}^3$. For all sinking probes, the Ladenburg correction is small [36]. Aluminum rods attached to the intruders are 2 mm diameter are long enough to allow for tens of millimeter of travel of the intruder. The weight of the rod was 1.74 grams for the cylinders and 2.24 grams for the sphere. The position of the intruder is measured using an traveling telescope with a vernier scale; timing is done using a digital stop watch. Readings are taken at one minute intervals. The error in position is set by the speed $\dot{\delta}$ at the time of the reading.

Packing preparation — The hydrogel packings are prepared by mixing a known weight of dry hydrogel powder (JRM Chemicals) with 2 liters of Oxford tap water, which has a pH of about 8 [35] and contains about 5 ppm sodium. Both pH and salinity affect hydrogel swelling characteristics [24, 25]. The water is boiled three times to remove dissolved gases; this method is an effective way of reducing the number of bubbles that might otherwise emerge in the sample. The water is cooled before mixing the dry hydrogel powder to create a low density sample. All measurements are carried out at $19 \pm 1 \text{ }^\circ\text{C}$ and the total liquid volume was also large enough to ensure temperature stability during an experiment. The mixture is stirred very slowly and allowed to settle for periods ranging from 2 to 4 days beneath a plunger which covered the entire surface. The plunger has a 380 gram weight attached to it so that each water/hydrogel sample was compressed to a dense packing by the same force before each run of the experiment, aiming for a protocol that ensures repeatability. It should be noted that the packing of particles always represents a settled bed. The frictionless nature of the particle interactions makes it very likely that the packing fraction is thus very close to random close packing at all times.

The hydrogel immersion in water all but removes the gravitational stress gradient, resulting in a gravitational

stresses of < 1000 Pa in our 20 cm tall sample as used in our experiment. We measure the position of the inserted intruder using the cathetometer during each run of the experiment. We checked repeatability by redoing the experiment after stirring the sample and allowing it to settle. To change the sample after each run, we use a jeweller's balance to measure out small quantities (typically ~ 0.1 grams) of dry hydrogel particles which are then mixed into the sample. All packings are thus characterized by a total concentration ρ grams of hydrogel per liter of water. Other intrusion experiments involve increasing the stress by adding weights to the tray.

Stress calculations — Note that when the intruder is totally submersed, we use the effective density ρ_{eff} of the intruder to compute the stress; ρ_{eff} depends on the density of the intruder. The addition of hydrogels also affects the average density ρ_{eff} , but this effect does not measurably affect the calculation of the stress. During the slow penetration of the intruder, the rod also slowly sinks into the hydrogel packing, gradually reducing the effective weight by $8 \mu\text{g}/\text{cm}$, which can be neglected on the total weight.

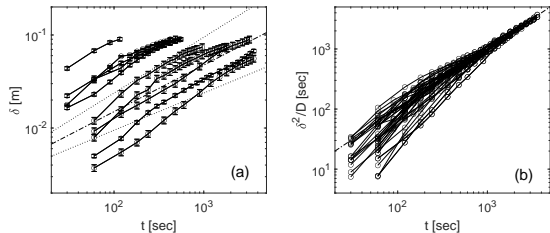


Figure 5. Reproducing Fig. 1(b),1(c) from the main article on double-logarithmic scales. (a) Penetration depth δ as a function of time for various hydrogel concentrations and added weights. The dash-dotted line has a slope of 0.5. The dotted lines have slopes of 0.4 and 0.6. (b) δ^2 dynamics normalized with fitted D values for all penetration tests. The dash-dotted line indicates a slope of unity.

Power law sinking rate — The power law nature of

the creep dynamics can be established in more detail by examining $\delta(t)$ and its rescaled variant on double-logarithmic plots. In Fig. 5 we show the same data as used for Fig. 1 of the main article on double-logarithmic scale. In Fig. 5a we include reference lines for different power law behavior to show that an exponent of 0.5 is very reasonable. The collapse shown in Fig. 5b indicates that during the first tens of seconds of the experiment, deviations may be observed from linearity, which are likely related to manual position measurement inaccuracies. The late time behavior, measured over several thousands of seconds, asymptotes to linearity on these rescaled axes.

Creep model — We use the framework for rheological constitutive equations for glassy and/or ageing materials described in [14, 37]. Taking a standard scalar Maxwell model as a starting point, the stress dynamics is set by relaxation via the “fluidity” and shear modulus

$$\dot{\sigma} = -f\sigma + G\dot{\gamma}, \quad (4)$$

where G is the elastic modulus and fluidity f is an inverse time associate with stress relaxation events. At the same time, $f(t)$ is described by the competition of an ageing process, increasing the characteristics relaxation time, and a rejuvenation process driven by shear. For the sinking ball experiments we can write that $\dot{\sigma} = 0$ and the observation is that $\delta(t) \propto t^{1/2}$ hence $\dot{\gamma} \propto t^{-1/2}$, although the scalar approach is not immediately justified. Substituting this, we find that $\sigma = t^{-1/2}G/f$ from which follows that $f \propto t^{-1/2}$ as the stress is held constant. With this in mind, the general form for $\dot{\gamma}$ as described by Derec *et al* becomes of interest:

$$\dot{f} = \left(r + u \left(\frac{\sigma f}{\dot{\gamma}} \right)^\lambda \frac{\dot{\gamma}^{\nu-\epsilon}}{f^\nu} \right) f^\alpha - v f^{\alpha+\beta}, \quad (5)$$

where all prefactors and exponents are positive constants whose magnitude determine the strength and type of aging and rejuvenation observed. For the hydrogel packing, we find $\dot{f} \propto t^{-3/2}$ hence one natural choice is $\alpha = 3$.